Application of imaging TOF-SIMS in cell and tissue research

KATRIN RICHTER

GÖTEBORG UNIVERSITY

Institute of Biomedicine

Department of Medical Biochemistry and Cell Biology

The Sahlgrenska Academy

Göteborg, Sweden 2007

ABSTRACT

This thesis is aimed at extending the use of TOF-SIMS (time of flight secondary ion mass spectrometry) as an analytical tool in cell and tissue research. TOF-SIMS is a relatively new method that allows analysis of the chemical composition of sample surfaces. Originally, it was used for imaging the distribution of elements on surfaces in materials science. Technical improvements have made analysis of fragile biological samples possible through localization of relevant secondary ions, e.g. lipid fragments and inorganic ion patterns. TOF-SIMS has several advantages over alternative imaging methods e.g. its sensitivity to all elements, detection of all isotopes, and it allows composite imaging of the surface distribution of detected elements and molecules.

The present work comprises new applications of cryomethods for preparation of TOF-SIMS tissue samples in an effort to obtain analytical results that reflect the vital situation as closely as possible. Lipid species (galactosylceramides, sulfatides or fatty acids) and ions (Na/K) were identified and localized in specimens from cerebellum, kidney and intestine with instruments equipped with a bismuth cluster primary ion source.

Two sample preparation sequences were employed: (i) plunge freezing in liquid nitrogen and cryosectioning; (ii) high-pressure freezing followed by freeze-fracturing and freeze-drying. The two preparation methods resulted in similar distributions of lipids and fatty acids but only sample preparation with high-pressure freezing allowed demonstration of separate distributions of sodium and potassium in rat cerebellum and kidney.

TOF-SIMS analysis revealed specific distributions of lipids cholesterol, phosphocholine, sulfatides, two galactosylceramide species and ions sodium and potassium in rat cerebellum. It could be shown that the white matter is separated into a "cytoplasm-rich" compartment containing phosphocholine, Na^+, K^+ and N-lignoceroylgalactosylceramide and a cholesterol-rich compartment containing cholesterol and N-stearoyl-galactosylceramide. Sulfatides with short chain fatty acids displayed a uniform distribution in the white matter and a patchy distribution for sulfatide with C24 fatty acids.

Fatty acid signals showed high intensities for stearic acid in Purkinje cell bodies of the rat cerebellum; the fatty acids palmitic and oleic acid displayed most intense signals located to the molecular and granular layer. Fatty acid imaging in mouse intestine revealed highest palmitic acid signals in the secretory crypt cells and the intestinal lumen and highest oleic acid signals in intestinal villi.

New data on the cellular and subcellular distribution of lipid molecular species in tissues have been presented that are not possible to achieve with other microscopical techniques. It is concluded that TOF-SIMS at the present state is a powerful tool in imaging of ions and organic compounds at a MW up to ≈ 1,000 in biological tissues. TOF-SIMS has a potential to provide very significant information for the understanding of physiological functions and pathological processes in biomedical research. Further technical development will extend the range of applications.

Key words: TOF-SIMS, imaging mass spectrometry, cryopreparation, ions, lipids, galactosylceramide, sulfatide, fatty acids

ISBN 978-91-628-7299-1 Göteborg 2007

to my parents

CONTENTS

LIST OF PAPERS

This thesis is based on the following papers, which will be referred to in the text by their roman numerals:

I Börner, K., Nygren, H., Hagenhoff, B., Malmberg, P., Tallarek, E. & Mansson, J. E.
Distribution of cholesterol and galactosylceramide in rat cerebellar white matter
Biochimica et Biophysica Acta 1761(3): 335-44 (2006)

II Richter, K., Nygren, H., Malmberg, P. & Hagenhoff, B.
Localization of fatty acids with selective chain length by imaging time-of-flight secondary ion mass spectrometry
Microscopy Research and Technique 70(7): 640-7 (2007)

III Nygren, H., Börner, K., Malmberg, P., Tallarek, E. & Hagenhoff, B.
Imaging TOF-SIMS of rat kidney prepared by high-pressure freezing
Microscopy Research and Technique 68(6): 329-34 (2005)

IV Pernber, Z., Richter, K., Mansson, J. E. & Nygren, H.
Sulfatide with different fatty acids has unique distributions in cerebellum as imaged by time-of-flight secondary ion mass spectrometry (TOF-SIMS)
Biochimica et Biophysica Acta 1771(2): 202-9 (2007)

ABBREVIATIONS

BSA	bovine serum albumin
CGT	ceramide galactosyltransferase
CST	galactosylceramide sulfotransferase
EM	electron microscopy
EM PACT	high-pressure freezing machine
FITC	fluorescein iso-thio-cyanate
GalC	galactosylceramide
HPF	high-pressure freezing
LMIG	liquid metal ion gun
LN_2	liquid nitrogen
m/z	mass to charge ratio
ME-SIMS	matrix-enhanced SIMS
PBS	physiological buffered solution
PC1	principal component 1
PCA	principal component analysis
PtdIn	phosphatidylinositol
SIMS	secondary ion mass spectrometry
Sulph I	antibody to the antigens sulfatide and seminolipid
tc	total of secondary ion counts per image
TOF-SIMS	time-of-flight secondary ion mass spectrometry

INTRODUCTION

Imaging techniques that explore cell and tissue morphology also provide fundamental data when investigating metabolism, physiology and function. A main goal in biological and medical research is the identification, localization and quantification of chemical elements and complex molecules. In this thesis the *time-of-flight-secondary ion mass spectrometry* (TOF-SIMS) technique is used for imaging of cell and tissue chemistry. In particular, results after tissue sample processing by cryo-fixation are explored.

Secondary ion mass spectrometry SIMS

The SIMS technique was developed about 60 years ago and first used to analyze oxides and metals. Later, the idea was to provide spatially resolved information with SIMS and that it should be possible to build an ion-optical collection system, analogous to a lens used in the light microscope, preserving the spatial relationship of the desorbed ions, as reviewed by Benninghoven et al. (1987). This was the beginning of imaging SIMS, which has been improved extensively and used in a variety of operational modes (Pacholski and Winograd 1999; Lockyer 2007; McDonnell and Heeren 2007).

SIMS is a mass spectrometry technique in which material desorbed from a surface by energetic particle bombardment is analyzed. The main principle behind the SIMS technique is the use of a focused ion beam of primary ions, generated by a liquid metal ion gun (LMIG), which impinge upon the surface. The energy of primary ions is transferred by atomic collisions to the target atoms, thereby setting up a collision cascade. The primary ions set atoms in motion, both by direct collisions with atoms in the sample or indirectly by collisions of atoms already in motion with other target atoms (figure 1). The energy is transferred back to the surface which allows surface atoms and molecules of approximately the top 2-3 molecular layers to overcome their surface binding energy (Vickerman and Briggs 2001). The ejected or sputtered atoms and molecules from the target surface are termed secondary ions. While most secondary ions come off neutrally charged, also a small portion generated is ionized, which can be subsequently analyzed as positive or negative ions by their mass to charge ratio *m/z*.

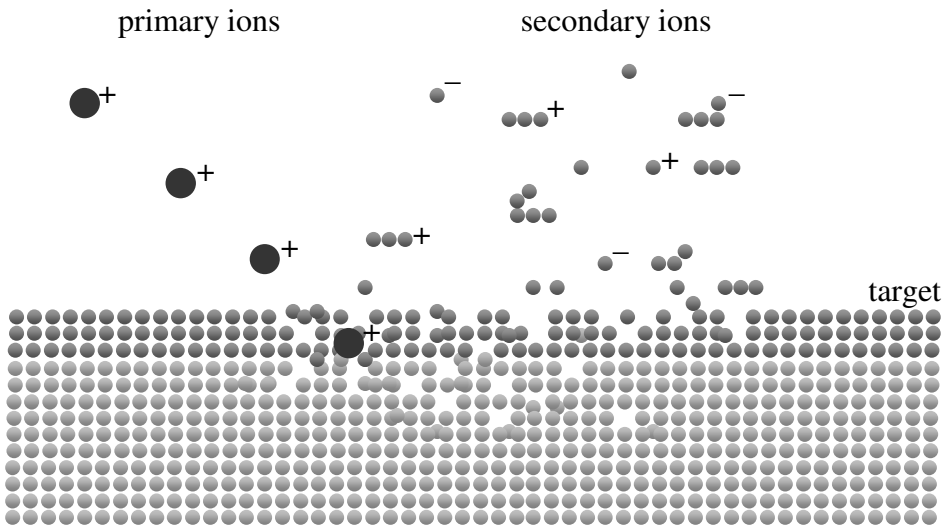

Figure 1: schematic drawing of the secondary ion emission process initiated by the impact of a primary ion

Depending on the ion dose, the technique can be separated into the two modes dynamic and static SIMS. In contrast to dynamic SIMS, static SIMS is performed with low primary ion doses. The surface density of atoms is typically 10^{15} atoms cm^{-2}. In static SIMS, less than 1% of the top monolayer is impacted by primary ions, yielding elemental and molecular distribution of secondary ions. The so-called static limit equates to a primary ion dose density of $<10^{13}$ cm^{-2} which results in sensitive analysis from the uppermost molecular layers with minimized sample damage. This setup also enabled desorption of larger organic fragments than in dynamic SIMS (Lockyer 2007). With the development of static SIMS, analysis of biological and biomedical material has become possible. Static SIMS for real surface analysis was first demonstrated by Benninghoven's group (Benninghoven 1994), who achieved major progress in the development of the time-of-flight secondary ion mass spectrometry technique.

Time-of-flight secondary ion mass spectrometry

TOF-SIMS is an acronym for the combination of the SIMS technique with Time of Flight mass analysis (TOF), which was first described in the 1980s (Chait and Standing 1981). The principle of TOF mass spectrometry is based on the fact that ions with different masses travel with different velocities. Basically, desorbed secondary ions from the target surface are accelerated by an electrostatic field and travel to the detector. The TOF analyzer separates the ions according to the time it takes for them to travel through the length of the field-free flight-tube (figure 2). This time interval is related to the mass and charge of the accelerated particles. The energy and angular dispersion of the secondary ions can be compensated using focusing elements such as a reflectron.

The lighter secondary ions arrive before the heavier ones whereby a mass spectrum can be recorded. The mass spectrum can then be used to obtain composition, distribution and molecular information of surface constituents (Belu, Graham et al. 2003).

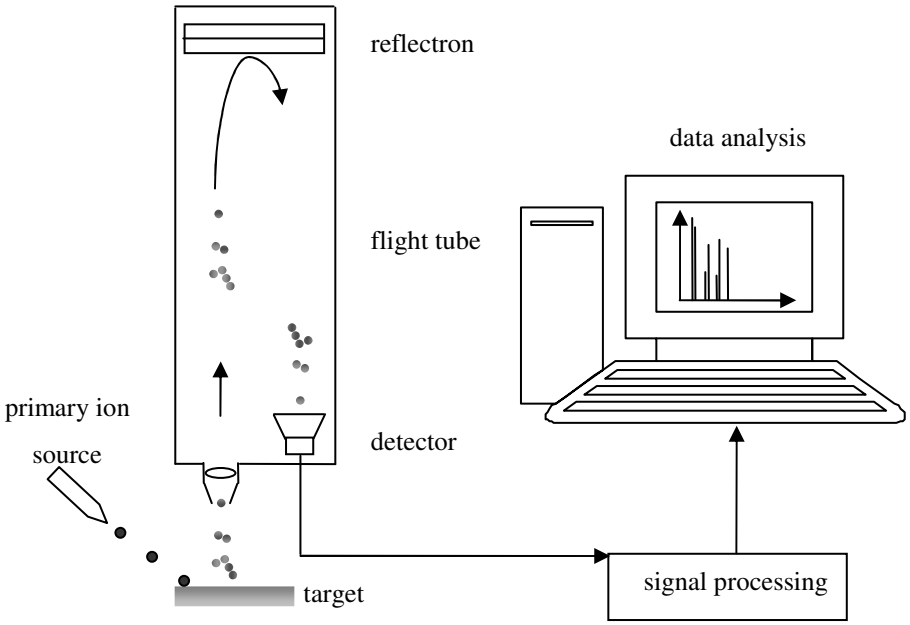

Figure 2: schematic drawing of a SIMS instrument with a TOF analyzer

With TOF-SIMS, spatially resolved images of molecular species with molecular weight up to several thousand Daltons and with a spatial resolution less than 100 nm can be produced (Schwieters, Cramer et al. 1991). Further, it allows parallel detection of multiple samples, excellent mass resolution, monolayer sensitivity and the ability to record the location of a wide range of atoms and molecules, including ions, lipids, and metabolites.

In TOF-SIMS, a pulsed primary ion beam is used which achieves greater specificity in mass-to-charge measurements (Benninghoven, Hagenhoff et al. 1993). The primary ion source can be operated in different modes of pulsing cycles, in which the pulse time defines the mass resolution. The shorter the pulse time, the higher is the mass resolution in the spectra. By "bunching" the raw pulse, high mass resolution with "narrow" peaks can be attained but with a spatial resolution lower than 2-5 µm. Thus, images obtained from spectra measured in the bunched mode appear often fuzzy. When the sample is analyzed at submicron spatial resolution, the primary ion gun is operated in a non-bunched mode, using longer pulse times of primary ion bombardment. This imaging or "burst alignment" mode allows for best spatial

resolution, which in turn is at a cost of the mass resolution (Sodhi 2004). The peaks in this mode appear broader, pooling several peaks which are located closely. It is therefore reasonable to measure the sample in both modes, gaining images in a good spatial resolution and allowing analysis of peaks in high mass resolution.

Improvements of TOF-SIMS in biological applications

The secondary molecular ion production is an important factor for resolution and quality of the image. The advancement of imaging TOF-SIMS was therefore associated with different methods of enhanced ion generation. The primary ion source largely determines secondary ion generation. For a long time the gallium primary ion source provided the best possible lateral resolution as compared to other sources, e.g. indium, argon, cesium or oxygen, making it the ion source of choice for high spatial resolution imaging MS experiments (Pacholski and Winograd 1999). Later on, gold cluster ions such as Au_2^+ and Au_3^+ have been shown to enhance the yield by more than ten-fold over gallium sources but the short lifetime of gold sources has been an issue (Andersen, Brunelle et al. 1998). With the use of gold primary ion sources the mass ranges were extended to imaging of secondary ions of higher masses which allowed imaging of e.g. cholesterol (Touboul, Halgand et al. 2004) as well as molecular species of phospholipids and sulfatides (Sjovall, Lausmaa et al. 2004) in tissues.

The next development step was the discovery that a LMIG providing polyatomic bismuth clusters yielded better intensities and efficiencies than the gold cluster LMIG. This allowed faster data acquisition times at submicron spatial resolution not attainable with gold primary ions sources (Nygren, Borner et al. 2005; Touboul, Kollmer et al. 2005). Other polyatomic primary ions e.g. C_{60}^+, (English, Van Stipdonk et al. 2001), SF_5^+ (Gillen and Roberson 1998) or highly charged atomic primary ions e.g. Au^{69+} (Schenkel, Hamza et al. 1999) have also been shown to significantly improve secondary ion yields but these are so far not available commercially.

Beside technical requirements, methods of post-ionization and chemical modification of the sample lead to enhanced sensitivity improving imaging TOF-SIMS measurements. After primary ion bombardment, only a small fraction of the desorbed material is ionized. With post-ionization, higher yields of charged organic fragments can be provided, e.g. with laser secondary neutral mass spectrometry (laser SNMS) (Arlinghaus, Fartmann et al. 2004; Dambach, Fartmann et al. 2004). Chemical modification techniques are based on deposition of ionization enhancing compounds, the “matrix”, e.g. dihydrobenzoic acid (DHB), or on sample

metallization. Matrix-enhanced SIMS (ME-SIMS) has been shown to increase secondary ion yield in brain tissue (Altelaar, van Minnen et al. 2005; McDonnell, Piersma et al. 2005). Sample metallization (Meta-SIMS), applying a nm-thick layer of gold or silver to the sample, has been shown to provide increased intensities for large analytes in biological tissue (Nygren, Malmberg et al. 2004; Altelaar, Klinkert et al. 2006). For a more detailed overview on ion generation the review article of McDonnell and Heeren (2007) is recommended.

Imaging TOF-SIMS

The chemical composition of a sample can be mapped by focussing the primary beam to a narrow diameter and scanning it across the surface. Different sizes of the area to be analyzed can be chosen, usually in the range from 10 x 10 to 500 x 500 μm^2 at a square-pixel density of 256 x 256, i.e. a pixel resolution of about 40 nm to 2 µm. Recently, the analysis area was extended up to 70 x 70 mm^2 as demonstrated by Smentkowski and Ostrowski (2007). A complete mass spectrum is obtained at each point in the raster of the ion beam. After data acquisition, a specific ion or a combination of ions can be selected by their mass to charge peaks from the spectrum and be presented as a surface distribution map (Belu, Graham et al. 2003). The images obtained thus represent signal intensities of one specific secondary ion, or several ions as combined colour-coded images.

Imaging TOF-SIMS on cells and tissues

The search for detailed knowledge on chemical organisation of cells and tissues is still developing in physiology and medicine. An overwhelming majority of imaging-based information concerns protein organisation. Therefore, an interesting and important property of the TOF-SIMS technology is that the yield of secondary ions covers a molecular range that includes inorganic ions, small organic species and fragments of larger biomolecules.

Accordingly, the information obtained has the potential to bridge an important gap in available imaging technologies by extending the range of demonstrable molecules to other fundamental building-stones than proteins, notably lipids, in cells and tissues. This is achieved as a direct analysis, i.e. without indirect procedures such as the ubiquitous immunocytochemistry[1].

---

[1]Immunohistochemistry is of limited value for the imaging of lipids, notwithstanding that significant achievements have utilized fluorescent stains, for example filipin-binding to choles-

terol (Gimpl and Gehrig-Burger 2007) or the localization of synthetic fluorescence-labelled lipids (Lester, Olds et al. 1994; Kuerschner, Ejsing et al. 2005).

It can also identify added organic compounds including isotopes and isotope-labelled species. Some recent progresses in this field are compiled in the following paragraphs.

In biomedical research, the first studies with imaging TOF-SIMS concerned the localization of drugs and isotopes in tissue. For example, a study was presented that examined the biodistribution of a radioactively labelled drug molecule targeting melanoma cells. The signals of the isotopes could be localized to the cytoplasm of melanoma cells and tumour-infiltrating macrophages as well as the cytoplasm of normal melanocytes in the pigmented structures of the skin and the eye (Chehade, de Labriolle-Vaylet et al. 2005). The renal distribution of ^{26}Mg (Chandra and Morrison 1997), the localization of anticancer drugs (Guerquin-Kern, Coppey et al. 1997) and the investigation of intra-and extracellular boron distributions in mouse kidney after treatment with boron-containing drugs (Arlinghaus, Fartmann et al. 2004) are further examples on topics for early TOF-SIMS studies in the biomedical field.

With the development and improvement of the technique e.g. the introduction of polyatomic bismuth source, the increase of secondary ion generation allowed imaging of organic analytes of high masses and at a high spatial resolution whereby TOF-SIMS applications were brought into the field of lipid research (Nygren and Malmberg 2007). For example, assembling of lipids was studied in membrane models, exhibiting sphingomyelin located in cholesterol domains in membrane monolayer systems (McQuaw, Zheng et al. 2007).TOF-SIMS analyses of different phospholipid assemblies showed a strong enhancement in the yield of both the molecular and the dimer ion peaks of 1-oleoyl-2-palmitoyl-sn-glycero-3-phosphocholine (POPC) from the bilayered structure as compared to monolayers or disordered films. It was suggested that the molecular peak may be used as an indicator for changes in the membrane structure and for the presence of bilayer structures in cell and tissue samples (Prinz, Hook et al. 2007)

An interesting extension of the use of the TOF-SIMS technique was suggested by Kulp et al. They showed by multivariate statistics that individual cells from three different human breast cancer cell lines gave rise to different spectra (regardless of the fact that the origin of many peaks in the lower mass range was unknown) indicating that TOF-SIMS might become a tool in diagnostic evaluation of malignant cell phenotypes (Kulp, Berman et al. 2006). The

origin of individual cells was also reflected in a TOF-SIMS analysis of lipid composition in the outer leaflet of the plasmalemma of macrophages after different exposure to cholesterol (Ostrowski, Kurczy et al. 2007).

The first TOF-SIMS studies on imaging lipids in cells managed to visualize lipid fragments in the lower mass range, which were identified as phosphocholine and cholesterol (Colliver, Brummel et al. 1997; Roddy, Cannon et al. 2002). By the recent state of the technique, distributions of lipid fragments and molecules with still higher masses have been identified in various species and tissues. TOF-SIMS images, e.g. on fatty acids in songbird brain (Amaya, Monroe et al. 2007), sulfatides and phosphatidylinositol in mouse brain (Sjovall, Lausmaa et al. 2004), vitamin E in mouse brain (Touboul, Kollmer et al. 2005), fatty acids in rat retina (Amemiya, Tozu et al. 2004), phosphatidic acids in atherosclerotic plaque (Mas, Touboul et al. 2007) or di- and triacylglycerols (DAGs, TAGs) in human adipose tissue (Malmberg, Nygren et al. 2007) were shown.

In studies focussed on pathological events, new high-resolution information on spatial lipid location was obtained in different tissues. A study showed cholesterol redistribution in intestine after cholera toxin treatment. The high spatial resolution allowed imaging of the finding that increased amounts of cholesterol were located to the nuclei of enterocytes in the treated tissue (Borner, Malmberg et al. 2006). Another study showed specific accumulation of two glycosphingolipids in cutaneous and renal biopsies from patients with Fabry disease. The glycosphingolipids were found accumulated in the dermis and hypodermis, but showed weak signals in the epidermis and in biopsies from healthy volunteers. In kidney biopsies, an increase of glycosphingolipids signals was seen correlated to the severity code of the disease. Standard diagnostic tools in Fabry disease could result in false negative for specific cases and were insufficient concerning structural or quantitative information. High-resolution imaging TOF-SIMS showed to fill this gap by specific chemical imaging of the different cell layers (Touboul, Roy et al. 2007). TOF-SIMS analysis on muscle biopsies from mice with Duchenne muscular dystrophy distinguished different regions in the biopsy. Regions undergoing oxidative stress, degeneration, regeneration, and stable ones were identified according to their chemical composition (Touboul, Brunelle et al. 2005). Finally, high-resolution TOF-SIMS images on human aorta revealed that e.g. cholesterol and oxysterols are located to the elastic lamellae in the aortic wall. Cholesterol distribution in human atherosclerotic plaques was seen to be irregular but with signals that were mainly located in spots in the intima region

(Malmberg, Borner et al. 2007). These findings provided novel information that could not be obtained with other techniques.

Sample preparation

Sample preparation is of major concern for biological imaging experiments. Important properties of samples suitable for imaging TOF-SIMS are good morphological preservation, sample integrity under ion bombardment, minimal sample contamination, and minimal redistribution of diffusible species. In addition to these requirements, it is desirable that the preparation procedure is practical and productive for routine analysis (Lazof, Goldsmith et al. 1994; Pacholski and Winograd 1999). In reality, a compromise between tissue preservation as close to its natural state as possible, on one hand, and conditions for the measurement under high vacuum, on the other, has to be accepted.

Theoretically, analysis of freshly gained tissue would represent an ideal experimental setup, but the necessity of ultra-high vacuum for secondary ion mass spectrometry requires a sample preparation that ensures that the sample remains stable under these conditions. Such an increase of specimen stability could be obtained by fixation. Some advantages of chemical fixation for the structure of adsorbed protein films analyzed with TOF-SIMS (Xia and Castner 2003), in mapping of elements bound to macromolecules (Clerc, Fourre et al. 1997) as well as in localization of lipids in rat brain (Borner, Nygren et al. 2006) were reported. However, routine tissue fixation procedures for microscopy that include chemicals, e.g. glutaraldehyde influence the location and/or interlinkage of ions and molecules and accordingly alter the natural cell chemistry. An immunohistochemical study reported loss of radiolabelled lipids in tissue samples during chemical fixation and resin embedding (Maneta-Peyret, Compere et al. 1999) and a TOF-SIMS study on soybean leaves showed that ion distribution patterns of chemically fixed samples were not in agreement with the known physiological distribution. In contrast, samples prepared with cryofixation showed the expected distribution patterns (Grignon, Halpern et al. 1997). Some advantages of cryofixation concerning the preservation of cellular components have been shown by e.g. enhanced preservation of immunocytochemistry compared to chemical fixatives (von Schack, Fakan et al. 1993; Baskin, Miller et al. 1996; Tsuyama, Matsushita et al. 2003).

In the field of imaging mass spectrometry, specimen preparation by cryotechniques has gained great interest. Cryofixation methods have the advantage of fast sample preparation and fixation, preserving the tissue without the use of chemical additives. Different methods of plunge-freezing[2] together with freeze-fracturing were established for cultured cells (Colliver, Brummel et al. 1997; Chandra 2001; Roddy, Cannon et al. 2002; Wittig, Wiemann et al. 2005). Tissues have also been prepared by plunge-freezing followed by sectioning (Sjovall, Lausmaa et al. 2004; McDonnell, Piersma et al. 2005; Amaya, Monroe et al. 2007). Here, the dissected tissue was directly cryofixed with a cryogen, sectioned with a cryostat and dried at room temperature. Without cryoprotection, plunge freezing inevitably results in formation of some ice crystals. This problem is overcome to a large extent with high-pressure freezing (HPF). With this method, fresh and untreated tissue is frozen at high pressure (≈2000 bar) and high speed (jet-stream of LN_2) to a vitrified state, so-called amorphous ice (Studer, Michel et al. 1989). The great advantage is that even samples of a substantial volume (at least within one hundred μm from the samples surface) are well frozen (Shimoni and Muller 1998; Studer, Graber et al. 2001; Vanhecke, Graber et al. 2003) since the pressurized water behaves as if cryoprotecting agents were added. The method was developed for EM studies where the unsurpassed quality of ultrastructural morphology after vitrification was exploited. It is also well established that HPF improves the conditions for immunolocalization of "difficult" antigens in proteins, e.g. actin in angiosperm pollen (Hess, Mittermann et al. 1995), peptides, e.g. adrenomedullin (Yuchi, Suganuma et al. 2002), and lipids, e.g. myelin glycolipids (Kirschning, Rutter et al. 1998).

Part of the present thesis work was undertaken on the assumption that both intra- and extracellular composition in bulk tissue could be analyzed with TOF-SIMS by employing freeze-fracturing after HPF, thereby presenting a well preserved, new and pristine surface to the primary ion beam.

[2] The specimen is rapidly immersed at ambient pressure into a liquid cryogen, either LN_2, or a secondary cryogen with higher thermal dissipation capacity such as melting propane

AIMS

Considering the challenging potential of the TOF-SIMS technology to provide unique information on the detailed distribution of ions and molecules that are largely inaccessible for analysis with other microscopy techniques the overall aim of this thesis work was:

- to develop routines for TOF-SIMS as a tool for imaging cell chemistry in intact tissues and organs. This included the simultaneous exploration of two separate aspects:

- to develop and evaluate optimal tissue preparation for TOF-SIMS analysis based on *cryotechniques*

- to assess the possibility to obtain *biologically relevant information* with available TOF-SIMS instrumentation through identification and imaging of selected ions and lipids in a variety of tissues and organs after cryopreparation.

MATERIALS AND METHODS

Animal and tissue preparation

Cerebellum and kidney studies were made on male Sprague–Dawley rats (300 g). The rats were deeply anaesthetised by inhalation with Isofluran Baxter (Baxter Medical AB, Kista, Sweden) and euthanized by exsanguination via cardiac puncture according to the ethical guidelines of the University of Göteborg.

Cerebellum

The skin was removed and the cranium opened carefully. The cerebellum was harvested by transection of the connections with the brainstem. Under a stereomicroscope, remnants of the meninges and blood vessels were removed and the cerebellar hemispheres were separated from the vermis. The preparation was performed in ice-cold physiological buffered solution (PBS), 0.05 M and pH 7.4. Further preparation steps are described below.

Kidney

The kidneys were removed after cutting the renal vein and artery. The ureters were cut. For sectioning with the oscillating tissue slicer and following high-pressure freezing, the kidneys were divided transversely into two equal halves in ice-cold PBS. The samples prepared by punching for high-pressure freezing were taken from the cortical region of the kidney.

Intestine

For experiments on intestine we used 12-14 weeks old Balb/c mice. Mice were euthanized with CO_2 and cervical dislocation. About two centimetres of mouse duodenum were dissected and the chyme was ejected by carefully squeezing the tissue. Afterwards, the tissue samples were plunge frozen in liquid nitrogen and stored there until cryosectioning.

Oscillating knife microtomy

Preparation of slices from unfixed tissue was carried out in ice-cold PBS with a Leica VT1000S unit. The kidney halves or the cerebellar hemispheres were glued onto the sample holder with Roticoll® tissue glue and immediately embedded in 3 % agarose with low melting point, dissolved in PBS (Sigma-Aldrich, Germany) when it was almost hardened. A slice of 900 μm thickness was first cut and discarded. The following slices, which were used for high-pressure freezing, were cut at a 300–350 μm thickness setting.

High-pressure freezing

Sample preparation with high-pressure freezing (HPF) and freeze-fracturing was used in the work presented in *Papers I and III*. HPF was performed at 2000 bar and -196 ºC with liquid nitrogen spray using the EM PACT machine (Leica, Vienna) as described in detail by Studer et al. (2001). The freeze-fracture equipment available for this system was used. First, when a section was obtained, a smaller tissue sample of about 1.2 mm in diameter was immediately punched out from a region of interest. This cylindrical piece of tissue was placed in the freeze-fracture holder under stereomicroscope control. The holder design includes a bottom carrier with a copper ring on top, which invests the sample. With the help of the loading station, this sandwich like arrangement was placed into the loading device. This in turn was inserted into the instrument and the automatic burst pressure rise and freezing cycle was initiated. After training, the punching - loading – freezing sequence could be performed in about 30 sec. After cryofixation, the carriers were collected in the liquid nitrogen bath of the EM PACT.

Freeze fracturing and freeze drying

The high-pressure frozen samples were transferred onto a pre-cooled copper block in liquid nitrogen. With the help of a pair of forceps, the copper ring was removed from the carrier, which creates a fractured surface through the tissue. The samples were placed on the cold copper block and freeze-dried over night at 10^{-3} mbar (Warley and Skepper 2000). The samples were kept in a desiccator under vacuum until measurement with TOF-SIMS.

Plunge freezing

Sample preparation with plunge-freezing and cryosectioning was used in the work presented in *Papers I, II and IV*. After careful dissection, the tissue was cut into smaller blocks of about 3-4 mm. Such specimens were placed on aluminium foil and rapidly immersed into liquid nitrogen at ambient pressure.

Cryosectioning

Cryosectioning was performed at -23 ºC with a Leica CM3050S cryostat. The plunge frozen tissue blocks were attached without further chemicals but water on the tissue holder. Slices of 8-25 µm were cut, placed on an object slide and kept in the refrigerator. Before measurement, the samples were dried at room temperature and placed in a box with dry silica gel as desiccant for transportation.

Richardson stain histology

After measurement with TOF-SIMS, the mouse intestine slices (*Paper II*) were stained with Richardson stain (Richardson, Jarett et al. 1960). The Richardson dye stains for DNA, RNA, and nuclear acids in the nucleus as well as in the cytoplasm.

Immunohistochemistry

The immunohistochemical method applied in *Paper IV* has been described previously (Pernber, Molander-Melin et al. 2002). Briefly, perfusion fixed Sprague–Dawley rat cerebellum (lateral hemispheres) were cut (50 μm thick) with an oscillating tissue cutter. Permeabilization with 0.05 % Tween20 and blocking with 1 % bovine serum albumin (BSA) in PBS were performed overnight at 4 °C in a free-floating procedure with constant agitation. Indirect double immunolabelling started with incubation with the monoclonal mouse Sulph I (20 mg/l) antibody described by Fredman et al. (1988) (diluted in 0.01 % Tween20/ 1 % BSA/ PBS) overnight at 4 °C, followed by incubation with 1 % donkey serum for 30 min and the secondary anti-mouse FITC-conjugated antibody (diluted 1:500) for 3–4 h at room temperature. Sections were then incubated as above with the second antibody rabbit anti-Neurofilament 200, IgG fraction of antiserum (Sigma N 4142) (diluted 1:100), 1 % donkey serum and the anti-rabbit Texas Red-conjugated antibody (diluted 1:600). Single immunolabellings and controls, treated similarly to samples but with one antibody excluded at a time, were also performed. Rinsing in PBS was performed between each incubation step. Stained sections were viewed with a Nikon Eclipse E600 microscope equipped with a Bio-RAD MRC-1024 confocal laser scanning unit. Images were collected using Kalman 5 image processing software, limiting photon noise and optimizing the contrast.

TOF-SIMS analysis

References

Cholesterol, grade > 99 %, was purchased from Sigma-Aldrich, Sweden. The galactosylceramide reference sample was prepared from bovine brain and characterized as described previously (Mansson and Svennerholm 1982; Svennerholm, Bostrom et al. 1992). The reference samples were dissolved in C/M/W (C=Chloroform, M=Methanol, W=Water, 30:60:20, by volume) at a concentration of 100 pM and prepared by droplet deposition onto clean aluminium foil before mass spectrometry analysis. Surface spectra were taken as described below. Other references were adopted from the literature.

Measurement

The tissue sections, the freeze fracture samples, and references were analyzed with an IONTOF TOF-SIMS IV or an IONTOF TOF-SIMS V instrument. Both instruments were equipped with a bismuth liquid metal ion gun (Bi-LMIG). First, surface spectra were taken from an area of 100 x 100 μm^2 in order to identify the species present at the respective surfaces. Here, the bunched mode was used (high mass resolution, 3 µm lateral resolution). Both Bi_1^+ and Bi_3^+ primary ions were applied with target currents of 0.4 pA and 0.15 pA, respectively. In *Papers I-IV* results with the Bi_3^+ source only are presented. The high mass resolution and high mass accuracy allowed assigning sum formulas to peaks even in the high mass range up to *m/z* 1000. Subsequently, mass resolved secondary ion images were acquired in burst alignment mode using Bi_3^+ (nominal mass resolution, lateral resolution 300 nm). The target current was 0.1 pA. Surface spectra and image raw data files were obtained either in the positive or in the negative analysis mode, gaining analytical and spatial information of positively and negatively charged secondary ions. For data analysis the IONTOF programs IonSpec and IonImage were used to analyze the spectra and to create images from the raw data information. The analysis time for each area investigated ranged from about 15 min to 2 hours, depending on the gained secondary ion intensity in the image. Fields of view ranged from 113 x 113 μm^2 to 500 x 500 μm^2 and the pixel density was 256 x 256. The field of view is given in figure legends. The intensity bar shows relative intensities with the black colour representing low secondary ion signals and with increasing yields of secondary ion intensities per pixel the colours turned to red, yellow and finally white for highest yields. In each paper the images represent ion and lipid distributions of one or two samples, thus exhibiting a snapshot of the tissue chemistry of two or three molecular layers of this sample area. The secondary ion signals mirror the current state of the tissue. This includes tissue physiology, treatment, experimental setup and location at the instant of tissue fixation.

Correlation Analysis

Correlation analysis of image data (*Paper III*) were performed using scatter plots (Chambers, Cleveland et al. 1983). Scatter plots visualize the intensity histograms of two images in a two-dimensional way where the occurrence of intensity combinations is colour coded. Images with a high degree of correlation show scatter plots with a positive slope whereas anti-correlated data show negative slopes or localized spots in the upper left und lower right quadrant of the plot. As an additional means for correlation analysis, colour coded overlay images were plotted where the intensity of up to three images is colour coded in red,

green, and blue. Image positions where more than one original image has significant intensities appear in the respective mixed colours. Mixed colours turned out as the following: red and green to yellow, red and blue to purple, green and blue to light green.

Secondary ion line profiles, as shown in *Paper II*, were drawn with the line profile function of the IonImage program. An area of interest was chosen in the secondary ion image of one image, of which a line profile was drawn and supplemented with the line profile drawn from the same area chosen in the image of another secondary ion image.

Multivariate Statistics

To identify the main contrast mechanism in the images, shown in *Paper III*, a principal components analysis (PCA) (Brereton 2003; Nygren and Malmberg 2004; Miller 2005) was performed. As input, 30 images of the most intense peaks in the spectrum were used (each normalized to the pixel with the highest intensity). Care was taken to ensure that all contrasts present in the 800 images detected (*m/z* 1–800) were included in the input data. A principal component (PC) is a linear combination of the original mass images where the 1st PC contains the highest variation on the data, the 2nd PC the second highest variation etc. All PCs form an ortho-normal base system. The so called score plot of the 1st PC (PC1) therefore describes the main contrast in an image experiment. If an image, for example, is dominated by topographical effects, PC1 will describe mainly the topography. PCA is a mathematical tool the results of which need to be interpreted with respect to the original analytical question. By normalizing all images to PC1, one can separate the remaining image contrasts from the main contrast. Normalization to PC1 in *Paper III* was therefore used to enhance the remaining contrast and to compensate for possible topographic effects.

SUMMARY OF PAPERS

Tissue preparation

In *Paper I*, both tissue preparation methods were presented, i.e. plunge-freezing and cryo-sectioning of the tissue on one hand and high-pressure freezing, freeze-fracturing and freeze-drying on the other. The localization of Na^+ and K^+ was not separated in plunge-frozen and sectioned samples but lipid secondary ions showed specific distribution patterns. In samples frozen by high-pressure liquid nitrogen, some degree of ion separation of Na^+ and K^+ could be seen. The distribution of the lipid secondary ions of cholesterol, galactosylceramides, and phosphocholine displayed similar pattern for the respective structures in high pressure frozen samples of rat cerebellum as well as in plunge-frozen and sectioned samples (figures 3 and 5, *Paper I*). TOF-SIMS images on rat kidney prepared by high-pressure freezing (*Paper III*) showed distinctly different lateral distributions of Na^+ and K^+. In *Papers II* and *IV*, negative TOF-SIMS images of specimen from rat cerebellum and mouse intestine prepared with cryo-fixation by plunge freezing were presented, revealing specific ion distribution patterns of fatty acids and sulfatide.

To summarize, two cryo-preparation techniques suitable for TOF-SIMS analysis of lipids in tissues have been used. High-pressure freezing, as it was applied for TOF-SIMS sample preparations for the first time, produced minimal tissue perturbation, i.e. an object close to the vital state and allowed analysis of an unaffected fractured surface which resulted in separate imaging of the diffusible ions Na^+ and K^+. Topographic effects could occur due to the specimen's irregular surface. Plunge-freezing and cryosectioning exhibited, to a certain extent, suboptimal tissue preservation as for example seen for ion distributions but the samples are flat reducing the possible influence of topography.

Lipid and ion distributions

Paper I

In this work, positive mode TOF-SIMS images of specific secondary ions could be shown in different layers of rat cerebellum. The images displayed known lipids cholesterol and the phosphatidylcholine headgroup phosphocholine as well as glycosphingolipids identified as galactosylceramides (GalC) with chain length of C18 (N-stearoyl-galactosylceramide) and C24 (N-lignoceroylgalactosylceramide), which have not been imaged with respect to their lateral distribution in tissue before. The cryosections prepared by plunge-freezing revealed highest concentrations of both Na^+ and K^+ in the cortical areas and in "star-shaped" areas in the white matter. A co-localization was seen between phosphocholine and Na^+/K^+, which was complementary to the distributions of cholesterol in "ribbon-shaped" areas in the white matter region. The white matter was seen to be separated into a "cytoplasm-rich" compartment containing phosphocholine, Na^+, K^+, and GalC C24 and into a cholesterol-rich compartment containing cholesterol and GalC C18. The distributions of GalC C18 and C24 were seen as dots, GalC C18 was located mainly in the white matter, whereas the GalC C24 signal extended also into the inner granular layer.

For high-pressure frozen, freeze fractured, and freeze dried samples some degree of ion separation of Na^+ and K^+ could be seen. With this preparation, areas without detectable amounts of phosphocholine were seen as 10-15 µm dots in the granular layer and as "ribbon-shaped" areas, 10-20 µm wide in the white matter but these areas in turn revealed cholesterol signals. The location of GalC C24 was clearly separate from the distribution of GalC C18 as seen in the overlay images.

Paper II

In this work, negative mode TOF-SIMS images on locations of fatty acids to specific cell types were displayed in samples from rat cerebellum and mouse intestine. The studied neural tissue revealed specific secondary ion distribution patterns of palmitic acid, oleic acid, and stearic acid with characteristic signal intensities in the different cerebellar layers. In the Purkinje cell layer and granular layer, palmitic acid and oleic acid secondary ions showed higher signal intensities than in white matter regions. Palmitic acid signals were low in cell body regions, whereas the oleic acid signal distribution showed the opposite pattern. In the white matter, the secondary ions of the saturated fatty acids palmitic and stearic acid showed lowest

signal intensities, whereas the unsaturated oleic acid was seen in 10-20 µm spots of higher intensities. At Purkinje cells bodies, high intensity spots of stearic acid secondary ions were observed around the cell nucleus. Spectral analysis of positive mode recordings revealed fragments of phosphatidylcholine in the same areas that displayed high intensity signals of stearic acid at the Purkinje cell body. Fragments of other phospholipids, like phosphatidylethanolamine, phosphatidylserine, and phosphatidylinositol were devoid or present in low intensity.

The second test tissue, the duodenum, displayed negative mode TOF-SIMS images on specific fatty acid distributions in mouse intestine. The secondary ions of palmitic acid revealed strongest signal intensities in the crypts of Lieberkühn. The intestinal lumen and the villi showed palmitic acid signals, which were lower in intensity than in crypt cells and which decrease towards the distal part of the villi. For linoleic acid, oleic acid, and stearic acid the highest intensity signals were seen within the intestinal villi. A gradient of signal intensity was observed for linoleic acid, lowest in the region around the crypts and highest at the distal part of the villi pointing to the lumen. Stearic acid was seen overall, with no specific localization sites. The secondary ions imaging the head group of phosphatidylinositol displayed highest intensities in the crypt region and in areas located to villus cells, the enterocytes.

Paper III

In *Paper III* positive mode TOF-SIMS images on inorganic ion distributions in the renal cortex of the rat kidney were collected. Two glomeruli, where the primary urine is filtered into the urinary space, could be identified. Proximal and distal tubules were seen located between the glomeruli and a larger collecting duct, where Na^+ is known to be re-adsorbed. The lateral distribution of Na^+ was distinctly different from that of K^+ and the phosphatidylcholine headgroup. Potassium was seen located within cells of the proximal tubulus epithelium and within cells of the glomeruli. High signals of sodium ions were seen within some cells of the distal tubulus epithelium, in the basal part of tubular epithelial cells, within the epithelium of the collecting ducts, and within the glomeruli. Phosphocholine was highest in areas where the sodium signal was low, which was expected assuming that sodium ions are localized in the interstitium.

Paper IV

The results of *Paper IV* showed that intensities of sulfatide species of different fatty acid chain length and hydroxylation were different within regions of the cerebellum, white matter, granule cell layer, Purkinje cell layer, and molecular layer. Cholesterol signals often formed long and narrow bands that identified the white matter, due to the high content of cholesterol in myelin. The TOF-SIMS analyses of individual sulfatide species revealed differences between white matter and the granule cell layer in 6/18 analyzed species. Sulfatide with the hydroxylated fatty acid chain Ch16:0 was the only molecular species that showed exclusive signal in the white matter. Sulfatide C24:1, C24:0, Ch24:0 in particular but also Ch22:0 and Ch24:1/C25:0 gave stronger signals from the granule cell layer as compared to the white matter. The other sulfatide species showed equal signals in the white matter and in the granule cell layer. The images with higher magnification (113×113 μm^2) of the white matter showed a patchy pattern, especially obvious with sulfatide C24:1, C24:0 and Ch24:0. These sulfatide patches were devoid of cholesterol signal. The anti-sulfatide antibody did neither label the molecular layer in cerebellum nor the Purkinje cells. The granule cell layer showed staining in both the neuropil and the granule cells and the white matter was very intensely stained.

DISCUSSION

Tissue preparation

A variety of plunge-freezing procedures to obtain a cryofixed specimen are available and this has become a widely used principle for TOF-SIMS sample preparation. In *Papers I, II and IV* we adopted this methodology. It was noted that the chemically unfixed samples prepared with this method had sufficient stability after dehydration to allow the high-vacuum analysis. Further, cryosections of plunge-frozen tissue were, in contrast to fractured high-pressure frozen samples, assumed to be flat which should be an advantage for TOF-SIMS analysis by reducing topography effects (discussed further below). Plunge frozen dried tissue showed specific distribution patterns of lipids at the single cell level, which indicates that this tissue fixation is suitable for TOF-SIMS analysis (*Papers I+II+IV*). However, plunge-frozen and sectioned specimens failed to maintain specific and separate distributions of ions (*Paper I*). Probably this reflects that unbound ions in interstitial water and the cytoplasm were redistributed during preparation. This might be expected since no cryo-protectants were used for reduction of ice crystal formation during freezing. Moreover, the warming of the tissue before cryosectioning to -23 °C likely caused further re-crystallization of water in the cells. Finally, the sections were thawed before drying at room temperature, which allows for redistribution of soluble material. Therefore, the TOF-SIMS results on cryosections were conceivably most relevant for localization of lipids at low resolutions since redistributions at smaller scale of length could not be excluded.

High-pressure freezing, the second method in the present thesis, was applied on tissue preparation for TOF-SIMS for the first time. The EM PACT freezing machine used in this study, achieves cooling rates of about 7000 °C s^{-1}, which is classified as very high cooling rates (Yavin and Arav 2007). In a study on cryofixation of *Saccharomyces cerevisiae* a cooling rate of more than 5000 °C min^{-1} was shown to prevent water exit from cells and thereby preserved the cell viability. This process seemed to be exponential, the higher the rate, the more the cell viability increased (Dumont, Marechal et al. 2003). In addition to the advantages of HPF for preservation of subcellular morphology, the cited viability assessments therefore support the assumption that the cellular distribution of water and solutes could be maintained through the EM PACT preparation of tissue samples. It should be emphasized that the TOF-SIMS analyses were performed on the fracture plane through the central part of the tissue blocks. This was a level at a good distance from the surfaces that were cut by the knife of the

oscillating slicer. Further, sample handling and preparation were carried out as rapidly as possible and under cold conditions in a physiological buffer solution.

According to these considerations, the adoption of the HPF technique followed by freeze fracturing should provide tissue specimens for TOF-SIMS analysis that reflect the intravital situation as closely as possible at the present state of technology. This is corroborated by the observation in nerve tissue and kidney that the ions sodium and potassium had separate distribution patterns (*Papers I + III*). The functional significance of the ion distribution patterns is supported e.g. by the particular finding of high levels of sodium in the basal part of renal tubular epithelial cells, displayed in TOF-SIMS images of this work (*Paper III*) This is consistent with earlier findings described in the literature which showed that renal epithelial cells are functionally polarized. Immunohistochemical studies revealed that the Na,K-ATPase resides at their basolateral surface which in turn generates a sodium gradient by active transport of sodium ions out of the cells into the basal interstitium (Caplan 2001). This could explain high sodium levels in the basal part of epithelial cells seen in the TOF-SIMS image figure 5, *Paper III*.

As indicated above, an advantage of cryotechniques for tissue fixation is the possibility to perform freeze-fracturing. Fracturing exposes a fresh surface that has not been in contact to the preparation environment. During the process of freeze-fracturing, the fracture runs at a random level through the tissue, breaking the frozen tissue into two parts. The analysis of the tissues in this thesis was not performed in image resolutions that allowed visualization of different fracture faces but the formation of fracture planes should be born in mind when interpreting the secondary ion distributions. The cryofracture preferentially follows the plane between the hydrophobic zones of the lipid bilayers in cellular membranes, often jumping from one bilayer to another. Moreover, by removing ice the freeze-drying step exposes additional membrane surfaces that had not been cleaved by the fracture (Branton 1966). Thus, both aspects of the inner as well as the outer leaflet of a membrane could be exposed to the ionic beam during TOF-SIMS analysis. Although it has been shown that lipids move between the inner and outer leaflet (Bevers, Comfurius et al. 1999), it is widely accepted that the lipid composition of the membrane bilayer in living cells is asymmetric. For example, a study on a Schwann cell line reported that the phospholipids of the plasma membrane of intact cells and of isolated plasma membrane fractions revealed asymmetric distribution. Sphingomyelin and phosphatidylcholine were preferentially located in the outer leaflet, while aminophospholipids

as phosphatidylethanolamine, phosphatidylserine, and phosphatidylinositol were preferentially seen in the inner leaflet of the membrane (Calderon and DeVries 1997). Although the fracture often follows the membrane, it also exposes volume compartments as e.g. the cytosol, the nucleoplasm, vesicles, and the extracellular space. It is, without further histological investigations, difficult to draw conclusions on which membrane surfaces exactly were imaged when considering their chemistry. In this thesis conclusions regarding the site of origin of specific signals are thus based on probability reasoning. Obviously, much further research, encompassing correlation with other high resolution techniques, are required to determine unequivocally the biological source of isolated organic ion signals that approach the resolution limit of the TOF-SIMS instrument (Nygren and Malmberg 2007).

Water can be a source of interference in TOF-SIMS analysis because water clusters dominate the mass spectra (Zierold and Schafer 1988; Colliver, Brummel et al. 1997; Roddy, Cannon et al. 2002; Roddy, Cannon et al. 2002). This necessitated a dehydration step, which was performed as freeze-drying for the high-pressure frozen samples and with drying at room temperature for the plunge-frozen and sectioned ones. Freeze-drying was accomplished according to the procedure described by (Warley and Skepper 2000). These authors reported that ion redistributions occurred below a distance of 40 nm from the specimen surface. Thus, ion redistributions are unlikely to have affected our results since only the most superficial volumes of the fractured samples were measured. Freeze-dried samples are known to undergo a certain amount of shrinkage, which we accepted as an unavoidable artefact in sample preparation for vacuum-dependent imaging techniques, cf. scanning electron microscopy (Boyde and Maconnachie 1981).

Data interpretation

In TOF-SIMS studies concern is directed to the possible influence of topography effects. In the context of the present work it is obvious that the surface of fractured specimens by necessity exhibits certain topographic irregularities. As expected, slight topographic effects were seen in the images of high-pressure frozen and fractured tissue, in contrast to the findings from cryosections. As topography can influence the ionization yields in SIMS (McDonnell, Piersma et al. 2005), images were compensated by normalization of the specific ion images over the total ion image (*Papers I+III*) or by normalization of images against the first principal component (PC1) in multivariate image analysis (*Paper III*). Normalization is an established image processing method which consists of dividing the spectra at each pixel by the

total ion counts at that pixel to reduce interference from topographic or matrix effects from chemical differences (Tyler, Rayal et al. 2007). Normalization to PC1 (*Paper III)* was used to enhance the remaining contrast and to compensate for possible topographic effects. Kidney samples revealed, after normalization, areas without signals in TOF-SIMS images which were identified as urinary spaces and lumina of renal tubules. It is conceivable that these fluid filled spaces were emptied of their content, the primary urine, during freeze drying and therefore exhibited particularly strong effects of topography. Both preparation methods used in this thesis resulted in identical distribution patterns of the lipids galactosylceramide, phosphocholine, and cholesterol in rat cerebellum as it could be shown in *Paper I*, which leads to the assumption that irregularities in topography did not impair histological results.

Truly quantitative SIMS analysis of biological specimens is impossible due to fluctuations in secondary ion yields as a function of chemical composition. For example, the presence of one secondary ion may quench ionization of other molecular species. In the image this would lead to the recording of areas with lower signal intensity that thus underestimates the presence of the material *in vivo*. Such matrix effects are particularly prominent when chemical heterogeneities are present in the system (Harton, Zhu et al. 2007). In the current series of works, we assume that areas without any signals do not result from these effects. Absence of signal is interpreted as absence or presence at a concentration below the detection limit of the molecular species in that area since secondary ions of the same species were seen in adjacent histological domains with very similar overall composition. This is exemplified by the dot-like sulfatide distribution pattern that was obtained in rat cerebellar white matter (*Paper IV*). For reasons of simplicity we thus consider an image with a graded distribution pattern of signal intensities to provide its own control or reference, i.e. differences in different tissue compartments within an area analyzed are considered as true (whereas quantitative statements are not allowed).

Lipid and ion distributions

Three different tissue types, which are cerebellum, kidney and intestine, were investigated in the series of works included in this thesis. They were chosen as model-system representing specific composition and function. Cerebellum represents nerve tissue, containing high amounts of specific membrane lipids and was thus considered to be suitable for the study of lipid distributions. The kidney has among other functions importance in ion homeostasis and is thus an adequate model for ion imaging studies. The intestine was chosen for lipid and fatty

acid studies since the intestine plays an important role in lipid metabolism. These tissues have been investigated intense previously with other methods, which simplifies the correlation of secondary ion locations to known tissue morphology and physiological functions.

There is an obvious need to correlate the images recorded by the TOF-SIMS instrumentation, containing analytical information, with our knowledge of cell and tissue organisation as established by other microscopy techniques. The properties and limitations of imaging spectrometry often make these correlations very difficult and necessitate indirect reasoning as regards the identity of structures that give rise to or lack secondary ion signals. This is particularly obvious when reproducible signals are obtained near the resolution limits of the system. In the present series of works on whole tissues correlative microscopical analysis was restricted to two light microscopy techniques. The first one employed a routine tissue staining according to the method of Richardson (*Paper II*), which was applied to sections that had been subjected to TOF-SIMS analysis. The second one, specific confocal immunofluorescence was made on separate samples that had been processed with chemical tissue fixation (*Paper IV*). It is probable that the true identity of "interesting sites" could be improved by different measures including scanning electron microscopy on the complementary fragment after freeze fracture, and light and electron microscopy on adjacent sections, i.e. that share surface with the TOF-SIMS specimen. In the following paragraphs some selected aspects of the correlation problems between the present TOF-SIMS results, tissue organisation, and functional aspects, are discussed.

In *Paper I*, cholesterol and glycolipids in the white matter of rat cerebellum were localized. Cholesterol-rich areas were found excluding Na^+ and K^+ secondary ion signals, conceivably dominated by myelin. These areas to a large extent co-localized with regions with a dot-like distribution of galactosylceramides. Three possible explanations to this dotted pattern were suggested. The first interpretation was based on the fact that sphingolipids are synthesized in the Golgi complex and are active in the intracellular regulation of membrane trafficking. Therefore, the dots might represent intracellular vesicles (Holthuis, Pomorski et al. 2001).

The second interpretation referred to the organisation of specific membrane domains. Membrane microdomains representing lipid rafts, caveolae, and tight junction regions, have been identified in the myelin membrane (Debruin and Harauz 2007). Monoglycerolceramides tend to be concentrated in the outer leaflet of the plasma membrane together with cholesterol in the specific membrane domains designated as lipid rafts (Simons, Kramer et al. 2000; Ha-

yashi and Su 2004). The resolution of the images shown in *Paper I* was too low for the unequivocal demonstration of rafts with a postulated average diameter in the range of 100 to 200 nm, which were seen in a wide variety of mammalian cell types (Sangiorgio, Pitto et al. 2004). To be able to suggest that the galactosylceramide signals covering 0.8 – 1.5 µm demonstrate lipid rafts, we must assume that rafts are distributed in small clusters or that these structures are larger than anticipated.

Because TOF-SIMS images displayed co-localization of ions with the galactolipid GalC C24 inside the white matter region, the third explanation to their dot-like distribution could relate to ion channels. Sphingolipids have been reported to contribute to the stability of paranodal regions and ion channel clusters in myelinated nerve fibres (Susuki, Baba et al. 2007), which supports the relation of galactosylceramides to ion channels. A study on knockout mice that lack the enzyme ceramide galactosyltransferase (CGT), which synthesizes the sphingolipids galactosylceramide GalC and the sulphated galactosylceramide sulfatide, showed that normal clustering of Na^+ and K^+-channels is disrupted in the myelin (Ishibashi, Dupree et al. 2002). Another study on Na,K-ATPase, an enzyme located near ion channels in the plasma membrane, showed Na,K-ATPase immunoreactivity at the nodes of Ranvier of axons from the peripheral and central nervous system (Ariyasu, Nichol et al. 1985). Accordingly, we assumed that the galactosylceramides are located to the nodes of Ranvier in the white matter myelin, where ion channels were determined. The star-shaped areas of approximately 10–20 µm in size with high intensities of phosphocholine and GalC C24 in TOF-SIMS images seen in *Paper I* could therefore represent nodal and paranodal regions of white mater axons. Areas with absence of secondary ion signals of phosphocholine and GalC C24 but presence of GalC C18 and cholesterol signals described as ribbon shaped areas in the white matter may hence represent regions of the internodal myelin sheath.

In this context it is interesting that we found a patchy distribution pattern of sulfatides, as described in *Paper IV*, which resembled the distributions of GalC, described in *Paper I*. Studies on knockout mice incapable of synthesizing sulfatide through disruption of the galactosylceramide sulfotransferase (CST) gene but capable of synthesizing GalC (Honke, Hirahara et al. 2002), showed that it is especially the paranode that is affected. In the peripheral nervous system sulfatide has been shown, using high magnification confocal microscopy, to be concentrated to the region of the nodal complex adjacent to the nodal region, the paranode (Pernber, Molander-Melin et al. 2002). These facts favour the presumption that also sulfatide has a special function in the paranodal area of the myelin and that the patchy image produced

by TOF-SIMS reflects sulfatide located to the paranode in the myelin of the white matter. The regional close location or even co-localization to the paranode is expected, since sulfatides are synthesized from GalC with the CST enzyme galactosylceramide sulfotransferase.

The latter example shows that TOF-SIMS analysis reveals information on different stages of lipid metabolism. This was achieved by analysis of fragments and molecules in the positive and negative mode of the same sample or even the same area investigated. Since the TOF-SIMS technique analyzes fragments and molecules at the same time, it is difficult to reason whether the detected secondary ions demonstrate the molecule of origin or a fragment of another lipid. Therefore, analysis of the fragmentation pattern of reference spectra is crucial when spectra data are interpreted (Al-Saad, Siems et al. 2003; Touboul, Brunelle et al. 2006). Nevertheless, information on different lipid components and fragments give valuable information on their origin, as also discussed in the paragraph on fatty acid distributions presented in *Paper II*.

In *Paper IV,* TOF-SIMS images showed specific localization of sulfatide molecular species of different chain length in rat cerebellum. The myelin contains the highest amount of sulfatide in the brain (Norton and Autilio 1966; Norton 1981). Therefore the white matter of the cerebellum, which is mainly composed of myelinated nerve fibres, would be expected to show strong sulfatide signals. The confocal immunofluorescence image of sulfatide distribution as revealed by the Sulph I antibody (*Paper IV*), showed most intense and homogenous sulfatide labelling in the white matter and less labelling in the granular layer. This is in agreement with previous studies (Ishizuka 1997; Pernber, Molander-Melin et al. 2002; Molander-Melin, Pernber et al. 2004). In contrast to the homogenously distributed sulfatide signals seen by immunofluorescence on perfusion fixed, sectioned, and permeabilized tissue, our analyses with TOF-SIMS (after plunge-freezing and cryosectioning) showed a patchy sulfatide distribution with small, irregular very high signal areas surrounded by low signal areas within the white matter. Similar locations for sulfatide signals in the white matter of mouse cerebrum, imaged with TOF-SIMS, have been shown by (Sjovall, Lausmaa et al. 2004). The patchy distribution could be related to nodal and paranodal regions of the myelin, as discussed above. In addition to possible influences of the different specimen preparations the apparent contradiction between the spectroscopy and confocal images might partly relate to the fact that TOF-SIMS signals are derived from the very surface of the specimen whereas even confocal immunofluorescence is influenced by volume and scattering effects.

Albeit this might be an insufficient explanation to the differences it is difficult to envisage that the patchy TOF-SIMS signal of sulfatide was artefactually generated. Assuming that the patchy signal of long chain fatty acid sulfatides nevertheless originates from a homogeneous distribution of the molecules it is possible that the explanation can be found in the composition of the myelin. Speculatively, long chain fatty acid sulfatides could be less available for imaging by TOF-SIMS in the compact myelin than in the paranodes, where the myelin lamellae open up into cytoplasmic loops (Peles and Salzer 2000). However, there is no technical or biological support for this notion. We suggest that the finding of sulfatide heterogeneity is of biological significance, awaiting further studies with independent techniques.

In *Paper II*, fatty acid distributions of different tissues were analyzed by TOF-SIMS. So far, the relative concentrations of fatty acids could be shown e.g. in cell fractions (Kuksis 1984) or in studies on fatty acid related proteins (Veerkamp and Zimmerman 2001) but imaging of the fatty acid distribution in tissues has been limited. With the development of the TOF-SIMS technique the first efforts to image fatty acids were made by the group of Touboul et al. on rat cerebrum (Touboul, Kollmer et al. 2005) and mouse muscle tissue (Touboul, Brunelle et al. 2005). In *Paper II*, for the first time, fatty acid distribution patterns could be shown to be specific for different cell types and cell layers with respect to chain length or grade of saturation. These results reduce the scale of fatty acid detection from a general verification regarding specific cell layers to a level that allows allocation of local variations *within* these cell layers and at the single cell level.

The negative mode TOF-SIMS images presented in *Paper II* displayed spots of higher fatty acid concentrations, about 10– 20 µm in size, inside the white matter. These spots could be related to areas assumed as nodal and paranodal regions in the myelin sheath as they were discussed for distributions of galactosylceramides (*Paper I*) and sulfatides (*Paper IV*).

The possibility of imaging both positive and negative secondary ions of the same sample area with TOF-SIMS allowed the investigation for further lipid constituents. A region of interest, in this case the area containing the Purkinje cell body, was chosen. By spectra analysis in the opposite mode we were able to search for phospholipid headgroup fragments (positive mode) and fatty acids (negative mode) at the same area. This in turn allowed for suggestions on the origin of imaged fatty acids.

Positive phosphocholine fragments were shown to be localized at the Purkinje cell body (figure 3, *Paper II*). The main part of detected fatty acids were thus supposed to originate from membrane bound glycero-or sphingolipids. These findings indicate that Purkinje cells have a specific membrane structure, other than the surrounding cells. This could be coupled to the physiological functions of Purkinje cells, which play a central role in signal reception and transduction in the cerebellum.

In mouse intestine, different distributions for the fatty acids palmitic acid, linoleic acid, oleic, and stearic acid were shown. These were suggested to originate from membrane bound phospholipids or from the intestinal mucine, a viscous highly glycosylated gel layer located to the intestine lumen, which is known to be capable of binding fatty acids (Gong, Turner et al. 1990; Krause 2000). This is supported by the finding that signals of phosphorylinositol at *m/z* 241 were co-localized with signals of the fatty acid palmitic acid, suggesting that the high intensity signals in TOF-SIMS images of palmitic acid originated from membrane bound phospholipids. Phosphorylinositol is a fragment of the phosphatidylinositol (PtdIn) headgroup as shown in previous studies on reference samples with mass spectrometry (Ekroos, Chernushevich et al. 2002; Taguchi, Houjou et al. 2005). Phosphoinositide fatty acids have been shown to regulate the PtdIn 5-kinase, phospholipase C and protein kinase C activities in rectal epithelial cells, which could be one of its functions in duodenal epithelium too (Carricaburu and Fournier 2001). However, the recorded fatty acid signals can also originate from other membrane lipids as for example phosphatidylethanolamine, phosphatidylserine, and phosphatidylcholine.

Future perspectives

So far, the application of the TOF-SIMS technique in simultaneous imaging of a variety of ions and lipids in cells and tissues is a great advance in biomedical research. A desirable goal is to extend imaging at sub-cellular levels through improved high resolution qualities approaching electron microscopical detail. It is conceivable that such a development will depend on further refining of the TOF-SIMS equipment but also on extended and parallel use of techniques from the EM realm. This was done in the present work by exploiting HPF and freeze-fracturing. Much additional information at the EM level is to be extracted from fractured specimens. Moreover, variations of cryo-ultramicrotomy offer the possibility to obtain specimens that merge information from EM and TOF-SIMS.

Some progress has been made on development of methods and techniques for analysis of biological samples for TOF-SIMS in the hydrated state with measurement under cold conditions (Chandra and Morrison 1996; Colliver, Brummel et al. 1997; Lockyer and Vickerman 2004). Our experiences of HPF indicate that direct analysis of the frozen-fractured specimen would be possible to perform. A promising enhancement of advantages of these techniques could be cutting of the high-pressure frozen sample at low temperature and direct analysis in the high-vacuum chamber, as it has been likewise done with plunge-freezing by the group of Arlinghaus in Münster, Germany (Tyler, Rangaranjan et al. 2006).

Recent fields of interest in imaging TOF-SIMS, e.g. 3D reconstructions of cells imaged in numerous planes at high resolution in the subcellular level are promising developments (Fletcher, Lockyer et al. 2007; Nygren, Hagenhoff et al. 2007). With further progress of the technique, e.g. enhancement of ion generation, imaging of molecules and fragments in the higher mass range could be improved, since the secondary ion yields gained in the mass range $m/z > 1000$ are rather low at the present state, even at long acquisition times. Together with advancements in sample preparation and TOF-SIMS operation, imaging of highly interesting lipids as e.g. gangliosides at a spatial resolution similar to the EM level are soon within the reach.

Already at present, TOF-SIMS represents a part and parcel on the repertoire of imaging methods in cell and tissue research.

CONCLUSIONS

The two rapid cryofixation techniques applied in this thesis were shown to be suitable preparation methods for bulk tissue samples prior to TOF-SIMS analysis:

- plunge-freezing followed by cryostat sectioning enabled imaging and distribution analysis of lipids (galactosylceramides, phospholipids, sulfatides, cholesterol and different fatty acids) in rat cerebellum and mouse intestine

- high-pressure freezing followed by freeze fracturing and freeze drying preserved the tissue chemistry to also enable separate localization of the diffusible ions sodium and potassium in kidney and cerebellum

- imaging TOF-SIMS could reveal specific distributions of lipid building-stones in cells and tissues

- our work has extended the range of TOF-SIMS applications in biomedical cell and tissue research

.

ACKNOWLEDGEMENTS

A journey is easier when you travel together. This thesis is the result of four years of work whereby I have been accompanied and supported by many people. I would like to express my deep and sincere gratitude to everyone who contributed to attaining this destination by some means or other. In particular, I would like to thank:

Professor Håkan Nygren for accepting me as a PhD student and introducing me to the interesting field of imaging TOF-SIMS. I am grateful for your support and scientific guidance.

Dr. Per Malmberg, for all collaboration and scientific guidance during this thesis.

Professor Bengt R Johansson for support and guidance with your flair for scientific issues and academic writing.

All co-authors, especially *Dr. Birgit Hagenhoff* and *Dr. Elke Tallarek*, Tascon GmbH in Münster, Germany and *ass. professor Jan-Eric Månsson* and *Dr. Zarah Pernber*, Institute of Neuroscience and Physiology, Göteborg University, for productive and pleasant collaboration.

Laila Falk, Eva Lyche and *Carina Ejdeholm* for all their help with the administration work.

My former and present collegues for creating a friendly and stimulating working atmosphere. Thank you *Noushin, Karin, Cecilia, Ann, Farhan, Ellie, Mobina, Niklas, Ylva, Yun, Yvonne, Gunnel, Ulf, Hayde, Yongling* and *Madeleine*.

The *Tascon GmbH* is gratefully acknowledged for skilful assistance during the measurements and teaching me all the valuable tricks in data analysis and image processing.

This work has been supported by the grants from the Swedish National Research Council and the Swegene Project.

REFERENCES

Al-Saad, K. A., Siems, W. F., Hill, H. H., Zabrouskov, V., et al. (2003). "*Structural analysis of phosphatidylcholines by post-source decay matrix-assisted laser desorption/ionization time-of-flight mass spectrometry*." J Am Soc Mass Spectrom 14 (4): 373-82.

Altelaar, A. F., Klinkert, I., Jalink, K., de Lange, R. P., et al. (2006). "*Gold-enhanced biomolecular surface imaging of cells and tissue by SIMS and MALDI mass spectrometry*." Anal Chem 78 (3): 734-42.

Altelaar, A. F., van Minnen, J., Jimenez, C. R., Heeren, R. M., et al. (2005). "*Direct molecular imaging of Lymnaea stagnalis nervous tissue at subcellular spatial resolution by mass spectrometry*." Anal Chem 77 (3): 735-41.

Amaya, K. R., Monroe, E. B., Sweedler, J. V. and Clayton, D. F. (2007). "*Lipid imaging in the zebra finch brain with secondary ion mass spectrometry*." International Journal of Mass Spectrometry 260 (2-3): 121-127.

Amemiya, T., Tozu, M. and Ohashi, Y. (2004). "*Time-of-flight secondary ion mass spectrometry can replace histochemistry demonstration of fatty acids in the retina*." Japanese Journal of Ophthalmology 48 (3): 287-293.

Andersen, H. H., Brunelle, A., Della-Negra, S., Depauw, J., et al. (1998). "*Giant metal sputtering yields induced by 20-5000 keV atom gold clusters*." Physical Review Letters 80 (24): 5433-5436.

Ariyasu, R. G., Nichol, J. A. and Ellisman, M. H. (1985). "*Localization of sodium/potassium adenosine triphosphatase in multiple cell types of the murine nervous system with antibodies raised against the enzyme from kidney*." J Neurosci 5 (10): 2581-96.

Arlinghaus, H. F., Fartmann, M., Kriegeskotte, C., Dambach, S., et al. (2004). "*Subcellular imaging of cell cultures and tissue for boron localization with laser-SNMS*." Surface and Interface Analysis 36 (8): 698-701.

Baskin, T. I., Miller, D. D., Vos, J. W., Wilson, J. E., et al. (1996). "*Cryofixing single cells and multicellular specimens enhances structure and immunocytochemistry for light microscopy*." J Microsc 182 (Pt 2): 149-61.

Belu, A. M., Graham, D. J. and Castner, D. G. (2003). "*Time-of-flight secondary ion mass spectrometry: techniques and applications for the characterization of biomaterial surfaces*." Biomaterials 24 (21): 3635-53.

Benninghoven, A. (1994). "*Surface-analysis by secondary-ion mass-spectrometry (SIMS)*." Surf Sci (299): 246-260.

Benninghoven, A., Hagenhoff, B. and Niehuis, E. (1993). "*Surface Ms - Probing Real-World Samples*." Analytical Chemistry 65 (14): A630-A640.

Benninghoven, A., Rudenauer, F. G. and Werner, H. W. (1987). *Secondary ion mass spectrometry*. Chichester, UK, Wiley & Son.

Bevers, E. M., Comfurius, P., Dekkers, D. W. and Zwaal, R. F. (1999). "*Lipid translocation across the plasma membrane of mammalian cells*." Biochim Biophys Acta 1439 (3): 317-30.

Borner, K., Malmberg, P., Mansson, J. E. and Nygren, H. (2006). "*Molecular imaging of lipids in cells and tissues* " IJMS 260 128-136.

Borner, K., Nygren, H., Hagenhoff, B., Malmberg, P., et al. (2006). "*Distribution of cholesterol and galactosylceramide in rat cerebellar white matter*." Biochim Biophys Acta 1761 (3): 335-44.

Boyde, A. and Maconnachie, E. (1981). "*Morphological correlations with dimensional change during SEM specimen preparation*." Scan Electron Microsc 4 27-34.

Branton, D. (1966). "*Fracture faces of frozen membranes*." Proc Natl Acad Sci U S A 55 (5): 1048-56.

Brereton, R. (2003). Chemometrics: Data Analysis for the Laboratory and Chemical Plant. New York, John Wiley & Sons

Calderon, R. O. and DeVries, G. H. (1997). "*Lipid composition and phospholipid asymmetry of membranes from a Schwann cell line*." J Neurosci Res 49 (3): 372-80.

Caplan, M. J. (2001). "*Ion pump sorting in polarized renal epithelial cells*." Kidney Int 60 (2): 427-30.

Carricaburu, V. and Fournier, B. (2001). "*Phosphoinositide fatty acids regulate phosphatidylinositol 5-kinase, phospholipase C and protein kinase C activities*." Eur J Biochem 268 (5): 1238-49.

Chait, B. T. and Standing, K. G. (1981). "*A time-of-flight mass spectrometer for measurement of secondary ion mass spectra*." Int J Mass Spectrom Ion Phys 40 185-193.

Chambers, J., Cleveland, W., Kleiner, B. and Turkey, P. (1983). *Graphical Methods for Data Analysis*. Florence, Wadsworth.

Chandra, S. (2001). "*Studies of cell division (mitosis and cytokinesis) by dynamic secondary ion mass spectrometry ion microscopy: LLC-PK1 epithelial cells as a model for subcellular isotopic imaging*." J Microsc 204 (Pt 2): 150-65.

Chandra, S. and Morrison, G. H. (1996). "*A novel approach for imaging the influx of Ca2+, Na+, and K+ in the same cell at subcellular resolution. Ion microscopy imaging of stable tracer isotopes*." Ann N Y Acad Sci 779 295-8.

Chandra, S. and Morrison, G. H. (1997). "*Evaluation of 26Mg stable isotope as an in vivo tracer of magnesium transport for SIMS ion microscopy imaging studies*." J Microsc 188 (Pt 2): 182-90.

Chehade, F., de Labriolle-Vaylet, C., Moins, N., Moreau, M. F., et al. (2005). "*Secondary ion mass spectrometry as a tool for investigating radiopharmaceutical distribution at the cellular level: the example of I-BZA and (14)C-I-BZA*." J Nucl Med 46 (10): 1701-6.

Clerc, J., Fourre, C. and Fragu, P. (1997). "*SIMS microscopy: methodology, problems and perspectives in mapping drugs and nuclear medicine compounds*." Cell Biol Int 21 (10): 619-33.

Colliver, T. L., Brummel, C. L., Pacholski, M. L., Swanek, F. D., et al. (1997). "*Atomic and molecular imaging at the single-cell level with TOF-SIMS*." Anal Chem 69 (13): 2225-31.

Dambach, S., Fartmann, M., Kriegeskotte, C., Bruning, C., et al. (2004). "*ToF-SIMS and laser-SNMS analysis of apatite formation in extracellular protein matrix of osteoblasts in vitro*." Surface and Interface Analysis 36 (8): 711-715.

Debruin, L. S. and Harauz, G. (2007). "*White matter rafting--membrane microdomains in myelin*." Neurochem Res 32 (2): 213-28.

Dumont, F., Marechal, P. A. and Gervais, P. (2003). "*Influence of cooling rate on Saccharomyces cerevisiae destruction during freezing: unexpected viability at ultra-rapid cooling rates*." Cryobiology 46 (1): 33-42.

Ekroos, K., Chernushevich, I. V., Simons, K. and Shevchenko, A. (2002). "*Quantitative profiling of phospholipids by multiple precursor ion scanning on a hybrid quadrupole time-of-flight mass spectrometer*." Anal Chem 74 (5): 941-9.

English, R. D., Van Stipdonk, M. J., Diehnelt, C. W. and Schweikert, E. A. (2001). "*Influence of constituent mass on secondary ion yield enhancements from polyatomic ion impacts on aminoethanethiol self-assembled monolayer surfaces*." Rapid Commun Mass Spectrom 15 (5): 370-2.

Fletcher, J. S., Lockyer, N. P., Vaidyanathan, S. and Vickerman, J. C. (2007). "*TOF-SIMS 3D biomolecular imaging of Xenopus laevis oocytes using buckminsterfullerene (C60) primary ions*." Anal Chem 79 (6): 2199-206.

Fredman, P., Mattsson, L., Andersson, K., Davidsson, P., et al. (1988). "*Characterization of the binding epitope of a monoclonal antibody to sulphatide*." Biochem J 251 (1): 17-22.

Gillen, G. and Roberson, S. (1998). "*Preliminary evaluation of an SF5+ polyatomic primary ion beam for analysis of organic thin films by secondary ion mass spectrometry*." Rapid Communications in Mass Spectrometry 12 (19): 1303-1312.

Gimpl, G. and Gehrig-Burger, K. (2007). "*Cholesterol Reporter Molecules*." Biosci Rep in press

Gong, D. H., Turner, B., Bhaskar, K. R. and Lamont, J. T. (1990). "*Lipid binding to gastric mucin: protective effect against oxygen radicals*." Am J Physiol 259 (4 Pt 1): G681-6.

Grignon, N., Halpern, S., Jeusset, J., Briancon, C., et al. (1997). "*Localization of chemical elements and isotopes in the leaf of soybean (Glycine max) by secondary ion mass spectrometry microscopy: Critical choice of sample preparation procedure*." Journal of Microscopy-Oxford 186 51-66.

Guerquin-Kern, J. L., Coppey, M., Carrez, D., Brunet, A. C., et al. (1997). "*Complementary advantages of fluorescence and SIMS microscopies in the study of cellular localization of two new antitumor drugs*." Microsc Res Tech 36 (4): 287-95.

Harton, S. E., Zhu, Z., Stevie, F. A., Aoyama, Y., et al. (2007). "*Carbon-13 labeling for quantitative analysis of molecular movement in heterogeneous organic materials using secondary ion mass spectrometry*." Anal Chem 79 (14): 5358-63.

Hayashi, T. and Su, T. P. (2004). "*Sigma-1 receptors at galactosylceramide-enriched lipid microdomains regulate oligodendrocyte differentiation*." Proc Natl Acad Sci U S A 101 (41): 14949-54.

Hess, M. W., Mittermann, I., Luschnig, C. and Valenta, R. (1995). "*Immunocytochemical localisation of actin and profilin in the generative cell of angiosperm pollen: TEM studies on high-pressure frozen and freeze-substituted Ledebouria socialis Roth (Hyacinthaceae)*." Histochem Cell Biol 104 (6): 443-51.

Holthuis, J. C., Pomorski, T., Raggers, R. J., Sprong, H., et al. (2001). "*The organizing potential of sphingolipids in intracellular membrane transport*." Physiol Rev 81 (4): 1689-723.

Honke, K., Hirahara, Y., Dupree, J., Suzuki, K., et al. (2002). "*Paranodal junction formation and spermatogenesis require sulfoglycolipids*." Proc Natl Acad Sci U S A 99 (7): 4227-32.

Ishibashi, T., Dupree, J. L., Ikenaka, K., Hirahara, Y., et al. (2002). "*A myelin galactolipid, sulfatide, is essential for maintenance of ion channels on myelinated axon but not essential for initial cluster formation*." J Neurosci 22 (15): 6507-14.

Ishizuka, I. (1997). "*Chemistry and functional distribution of sulfoglycolipids*." Prog Lipid Res 36 (4): 245-319.

Kirschning, E., Rutter, G. and Hohenberg, H. (1998). "*High-pressure freezing and freeze-substitution of native rat brain: suitability for preservation and immunoelectron microscopic localization of myelin glycolipids*." J Neurosci Res 53 (4): 465-74.

Krause, W. J. (2000). "*Brunner's glands: a structural, histochemical and pathological profile*." Prog Histochem Cytochem 35 (4): 259-367.

Kuerschner, L., Ejsing, C. S., Ekroos, K., Shevchenko, A., et al. (2005). "*Polyene-lipids: a new tool to image lipids*." Nat Methods 2 (1): 39-45.

Kuksis, A. (1984). "*Quantitative and positional analysis of fatty acids*." Lab Res Methods Biol Med 10 77-131.

Kulp, K. S., Berman, E. S., Knize, M. G., Shattuck, D. L., et al. (2006). "*Chemical and biological differentiation of three human breast cancer cell types using time-of-flight secondary ion mass spectrometry*." Anal Chem 78 (11): 3651-8.

Lazof, D. B., Goldsmith, J. K. G., Rufty, T. W., Suggs, C., et al. (1994). "*The preparation of cryosections from plant tissue: An alternative method appropriate for secondary ion mass spectrometry studies of nutrient tracers and trace metals*." J Microsc 176 (2): 99-109.

Lester, D. S., Olds, J. L., Schreurs, B. G., McPhie, D., et al. (1994). "*Incorporation of fluorescent lipids into living rabbit hippocampal and cerebellar slices*." Neuroimage 1 (4): 264-75.

Lockyer, N. P. (2007). "*Static secondary ion mass spectrometry for biological and biomedical research*." Methods Mol Biol 369 543-67.

Lockyer, N. P. and Vickerman, J. C. (2004). "*Progress in cellular analysis using ToF-SIMS*." Applied Surface Science 231-232 377-384.

Malmberg, P., Borner, K., Chen, Y., Friberg, P., et al. (2007). "*Localization of lipids in the aortic wall with imaging TOF-SIMS*." Biochim Biophys Acta 1771 (2): 185-95.

Malmberg, P., Nygren, H., Richter, K., Chen, Y., et al. (2007). "*Imaging of Lipids in Human Adipose Tissue by Cluster Ion TOF-SIMS*." Microsc Res Tech 70 (9): 828-35.

Maneta-Peyret, L., Compere, P., Moreau, P., Goffinet, G., et al. (1999). "*Immunocytochemistry of lipids: chemical fixatives have dramatic effects on the preservation of tissue lipids*." Histochem J 31 (8): 541-7.

Mansson, J. E. and Svennerholm, L. (1982). "*The use of galactosylceramides with uniform fatty acids as substrates in the diagnosis and carrier detection of Krabbe disease*." Clin Chim Acta 126 (2): 127-33.

Mas, S., Touboul, D., Brunelle, A., Aragoncillo, P., et al. (2007). "*Lipid cartography of atherosclerotic plaque by cluster-TOF-SIMS imaging*." Analyst 132 (1): 24-6.

McDonnell, L. A. and Heeren, R. M. (2007). "*Imaging mass spectrometry*." Mass Spectrom Rev 26 (4): 606-43.

McDonnell, L. A., Piersma, S. R., MaartenAltelaar, A. F., Mize, T. H., et al. (2005). "*Subcellular imaging mass spectrometry of brain tissue*." J Mass Spectrom 40 (2): 160-8.

McQuaw, C. M., Zheng, L., Ewing, A. G. and Winograd, N. (2007). "*Localization of sphingomyelin in cholesterol domains by imaging mass spectrometry*." Langmuir 23 (10): 5645-50.

Miller, J. (2005). *Statistics and Chemometrics for Analytical Chemistry* Upper Saddle River, Pearson Prentice Hall.

Molander-Melin, M., Pernber, Z., Franken, S., Gieselmann, V., et al. (2004). "*Accumulation of sulfatide in neuronal and glial cells of arylsulfatase A deficient mice*." J Neurocytol 33 (4): 417-27.

Norton, W. T. (1981). "*Biochemistry of myelin*." Adv Neurol 31 93-121.

Norton, W. T. and Autilio, L. A. (1966). "*The lipid composition of purified bovine brain myelin*." J Neurochem 13 (4): 213-22.

Nygren, H., Borner, K., Hagenhoff, B., Malmberg, P., et al. (2005). "*Localization of cholesterol, phosphocholine and galactosylceramide in rat cerebellar cortex with imaging TOF-SIMS equipped with a bismuth cluster ion source*." Biochim Biophys Acta 1737 (2-3): 102-10.

Nygren, H., Hagenhoff, B., Malmberg, P., Nilsson, M., et al. (2007). "*Bioimaging TOF-SIMS: High resolution 3D imaging of single cells*." Microsc Res Tech in press

Nygren, H. and Malmberg, P. (2004). "*Silver deposition on freeze-dried cells allows subcellular localization of cholesterol with imaging TOF-SIMS*." J Microsc 215 (Pt 2): 156-61.

Nygren, H. and Malmberg, P. (2007). "*High-resolution imaging by organic secondary ion mass spectrometry*." Trends in Biotechnology in press

Nygren, H., Malmberg, P., Kriegeskotte, C. and Arlinghaus, H. F. (2004). "*Bioimaging TOF-SIMS: localization of cholesterol in rat kidney sections*." FEBS Lett 566 (1-3): 291-3.

Ostrowski, S. G., Kurczy, M. E., Roddy, T. P., Winograd, N., et al. (2007). "*Secondary ion MS imaging to relatively quantify cholesterol in the membranes of individual cells from differentially treated populations*." Anal Chem 79 (10): 3554-60.

Pacholski, M. L. and Winograd, N. (1999). "*Imaging with mass spectrometry*." Chem Rev 99 (10): 2977-3006.

Peles, E. and Salzer, J. L. (2000). "*Molecular domains of myelinated axons*." Curr Opin Neurobiol 10 (5): 558-65.

Pernber, Z., Molander-Melin, M., Berthold, C. H., Hansson, E., et al. (2002). "*Expression of the myelin and oligodendrocyte progenitor marker sulfatide in neurons and astrocytes of adult rat brain*." J Neurosci Res 69 (1): 86-93.

Prinz, C., Hook, F., Malm, J. and Sjovall, P. (2007). "*Structural effects in the analysis of supported lipid bilayers by time-of-flight secondary ion mass spectrometry*." Langmuir 23 (15): 8035-41.

Richardson, K. C., Jarett, L. and Finke, E. H. (1960). "*Embedding in epoxy resins for ultrathin sectioning in electron microscopy*." Stain Technol 35 313-23.

Roddy, T. P., Cannon, D. M., Jr., Meserole, C. A., Winograd, N., et al. (2002). "*Imaging of freeze-fractured cells with in situ fluorescence and time-of-flight secondary ion mass spectrometry*." Anal Chem 74 (16): 4011-9.

Roddy, T. P., Cannon, D. M., Jr., Ostrowski, S. G., Winograd, N., et al. (2002). "*Identification of cellular sections with imaging mass spectrometry following freeze fracture*." Anal Chem 74 (16): 4020-6.

Sangiorgio, V., Pitto, M., Palestini, P. and Masserini, M. (2004). "*GPI-anchored proteins and lipid rafts*." Ital J Biochem 53 (2): 98-111.

Schenkel, T., Hamza, A. V., Barnes, A. V., Newman, M. W., et al. (1999). "*Surface analysis by highly charged ion based secondary ion mass spectrometry*." Physica Scripta T80a 73-75.

Schwieters, J., Cramer, H. G., Heller, T., Jurgens, U., et al. (1991). "*High Mass Resolution Surface Imaging with a Time-of-Flight Secondary Ion Mass-Spectroscopy Scanning Microprobe*." Journal of Vacuum Science & Technology a-Vacuum Surfaces and Films 9 (6): 2864-2871.

Shimoni, E. and Muller, M. (1998). "*On optimizing high-pressure freezing: from heat transfer theory to a new microbiopsy device*." J Microsc 192 (Pt 3): 236-47.

Simons, M., Kramer, E. M., Thiele, C., Stoffel, W., et al. (2000). "*Assembly of myelin by association of proteolipid protein with cholesterol- and galactosylceramide-rich membrane domains*." J Cell Biol 151 (1): 143-54.

Sjovall, P., Lausmaa, J. and Johansson, B. (2004). "*Mass spectrometric imaging of lipids in brain tissue*." Anal Chem 76 (15): 4271-8.

Smentkowski, V. S. and Ostrowski, S. G. (2007). "*Time of flight secondary ion mass spectrometry: A powerful high throughput screening tool*." Rev Sci Instrum 78 (7): 072215.

Sodhi, R. N. (2004). "*Time-of-flight secondary ion mass spectrometry (TOF-SIMS):--versatility in chemical and imaging surface analysis*." Analyst 129 (6): 483-7.

Studer, D., Graber, W., Al-Amoudi, A. and Eggli, P. (2001). "*A new approach for cryofixation by high-pressure freezing*." J Microsc 203 (Pt 3): 285-94.

Studer, D., Michel, M. and Muller, M. (1989). "*High pressure freezing comes of age*." Scanning Microsc Suppl 3 253-68; discussion 268-9.

Susuki, K., Baba, H., Tohyama, K., Kanai, K., et al. (2007). "*Gangliosides contribute to stability of paranodal junctions and ion channel clusters in myelinated nerve fibers*." Glia 55 (7): 746-57.

Svennerholm, L., Bostrom, K., Fredman, P., Jungbjer, B., et al. (1992). "*Membrane lipids of human peripheral nerve and spinal cord*." Biochim Biophys Acta 1128 (1): 1-7.

Taguchi, R., Houjou, T., Nakanishi, H., Yamazaki, T., et al. (2005). "*Focused lipidomics by tandem mass spectrometry*." J Chromatogr B Analyt Technol Biomed Life Sci 823 (1): 26-36.

Touboul, D., Brunelle, A., Halgand, F., De La Porte, S., et al. (2005). "*Lipid imaging by gold cluster time-of-flight secondary ion mass spectrometry: application to Duchenne muscular dystrophy*." J Lipid Res 46 (7): 1388-95.

Touboul, D., Brunelle, A. and Laprevote, O. (2006). "*Structural analysis of secondary ions by post-source decay in time-of-flight secondary ion mass spectrometry*." Rapid Commun Mass Spectrom 20 (4): 703-9.

Touboul, D., Halgand, F., Brunelle, A., Kersting, R., et al. (2004). "*Tissue molecular ion imaging by gold cluster ion bombardment*." Anal Chem 76 (6): 1550-9.

Touboul, D., Kollmer, F., Niehuis, E., Brunelle, A., et al. (2005). "*Improvement of biological time-of-flight-secondary ion mass spectrometry imaging with a bismuth cluster ion source*." J Am Soc Mass Spectrom 16 (10): 1608-18.

Touboul, D., Roy, S., Germain, D. P., Chaminade, P., et al. (2007). "*MALDI-TOF and cluster-TOF-SIMS imaging of Fabry disease biomarkers*." International Journal of Mass Spectrometry 260 (2-3): 158-165.

Tsuyama, S., Matsushita, S., Nonaka, S., Yonezawa, S., et al. (2003). "*Cytochemistry of gastric parietal cells with high-pressure freezing followed by freeze-substitution*." J Electron Microsc (Tokyo) 52 (2): 145-51.

Tyler, B. J., Rangaranjan, S., Moller, J., Beumer, A., et al. (2006). "*TOF-SIMS imaging of chlorhexidine-digluconate transport in frozen hydrated biofilms of the fungus Candida albicans*." Applied Surface Science 252 (19): 6712-6715.

Tyler, B. J., Rayal, G. and Castner, D. G. (2007). "*Multivariate analysis strategies for processing ToF-SIMS images of biomaterials*." Biomaterials 28 (15): 2412-23.

Vanhecke, D., Graber, W., Herrmann, G., Al-Amoudi, A., et al. (2003). "*A rapid microbiopsy system to improve the preservation of biological samples prior to high-pressure freezing*." J Microsc 212 (Pt 1): 3-12.

Warley, A. and Skepper, J. N. (2000). "*Long freeze-drying times are not necessary during the preparation of thin sections for X-ray microanalysis*." J Microsc 198 (Pt 2) 116-23.

Veerkamp, J. H. and Zimmerman, A. W. (2001). "*Fatty acid-binding proteins of nervous tissue*." J Mol Neurosci 16 (2-3): 133-42; discussion 151-7.

Vickerman, J. C. and Briggs, D. (2001). *TOF-SIMS: Surface analysis by mass spectrometry.*, Chichester: IM Publications

Wittig, A., Wiemann, M., Fartmann, M., Kriegeskotte, C., et al. (2005). "*Preparation of cells cultured on silicon wafers for mass spectrometry analysis*." Microsc Res Tech 66 (5): 248-58.

von Schack, M. L., Fakan, S., Villiger, W. and Muller, M. (1993). "*Cryofixation and cryosubstitution: a useful alternative in the analyses of cellular fine structure*." Eur J Histochem 37 (1): 5-18.

Xia, N. and Castner, D. G. (2003). "*Preserving the structure of adsorbed protein films for time-of-flight secondary ion mass spectrometry analysis*." J Biomed Mater Res A 67 (1): 179-90.

Yavin, S. and Arav, A. (2007). "*Measurement of essential physical properties of vitrification solutions*." Theriogenology 67 (1): 81-9.

Yuchi, H., Suganuma, T., Sawaguchi, A., Ide, S., et al. (2002). "*Cryofixation processing is an excellent method to improve the retention of adrenomedullin antigenicity*." Histochem Cell Biol 118 (3): 259-65.

Zierold, K. and Schafer, D. (1988). "*Preparation of cultured and isolated cells for X-ray microanalysis*." Scanning Microsc 2 (3): 1775-90.

APPENDIX (PAPERS I-IV)